Supporting Information

Multifunctional copper-nitrogen/carbon laccase-mimicking nanozyme for colorimetric sensing of phenolic compounds and degradation of organic pollutants

Xu Liu[1], Hongtian Yang[2], Yide Han[1], Yufeng Liu[3], Ying Zhang[2], Wenhao Li[1]*, Xia Zhang[1]*

1. Department of Chemistry, College of Sciences, Northeastern University, Shenyang 110819, P. R. China.

2. Institute of basic medical sciences of Xiyuan Hospital, China Academy of traditional Chinese medicine, Beijing 100091, PR China.

3. College of Pharmacy, Liaoning University, Shenyang 110036, China

*Corresponding author.

Email: liwenhao@mail.neu.edu.cn and xzhang@mail.neu.edu.

1 Experimental section

1.1 Materials

N, N-dimethylformamide (DMF), methanol (MeOH), ethanol (EtOH) and isopropanol were purchased from Fuyu Fine Chemical Co. Ltd. (Tianjin, China). 2,2,6,6-tetramethylpiperidine (TEMP), 4-Chlorophenol, Phenol, 2,4-Dichlorophenol (2,4-DP), 4-Aminoantipyrine (4-AP), 1,10-Phenanthroline, o-Phenylenediamine (OPD), p-Benzoquinone (p-BQ), Dopamine (DA), Histidine (His) were obtained from Macklin Chemical Co. Ltd. (Shanghai, China). 2-(N-Morpholino) ethanesulfonic acid (MES) was purchased from Yuanye Bio-Technology Co., Ltd (Shanghai, China). Laccase and Horseradish peroxidase (HRP) were purchased from Aladdin Chemical Co. Ltd. (Shanghai, China).

1.2. Characterization

The morphology was observed by Field-emission scanning electron microscope (FESEM, Hitachi SU-8010, Japan). Transmission electron microscopy (JEM2100PLUS, JEOL, Beijing) was also employed to character morpholgy, particle sizes and the mass percentages of individual elements in the samples. The XRD patterns were recorded by using a PANalytical Empyrean X-ray diffractometer (Cu were collected by using a VERTEX 70 Fourier transform infrared spectrophotometer (Bruker, Germany). X-ray photoelectron spectra (XPS) were obtained using a Thermo Scientific K-Alpha+ electron spectrometer (Thermo Fisher) by using AlK alpha radiation. The UV-Vis absorption spectra were recorded by a TU-1901 UV-Vis spectro photometer (Persee, China). Electron paramagnetic resonance (EPR) measurements

were obtained by an EMXplus (Bruker, Germany). The element contents were obtained by inductively coupled plasma optical emission spectrometry (ICP-OES) (Avio 500) (Perkinelmer, United States).

1.3 Catalytic stability assessment

To determine the effects of pH values on catalytic activity, Cu-N/C nanozyme and free laccase were shaken at 25 °C for 40 min in different pH ranges (3 to 9) and their relative catalytic activity was determined by colorimetric reactions of 2,4-diaminophen (2,4-DP) and 4-aminoantipyrine (4-AP). Subsequently, thermal stability was assessed by incubating both catalysts at temperatures ranging from 25 to 85 °C for 40 min. The effect of salt concentration on catalytic activity was investigated by adding different concentrations (0–600 mM) of NaCl to the reaction system to evaluate the effect of ionic strength. In addition, the effects of different ethanol concentrations (0–100%) on the catalytic activity of Cu-N/C and free laccase were determined. Finally, to evaluate the cycling catalytic stability of Cu-N/C, the Cu-N/C suspension was mixed with 2,4-DP and 4-AP, and after shaking at 25 °C for 40 min, Cu-N/C was recovered by centrifugation for the next round of reaction.

1.4 Determination of reactive oxygen species (ROS)

To determine the reactive species potentially produced during the reaction, isopropanol (IPA), p-benzoquinone (p-BQ), histidine (His), and EDTA were used as scavengers of ·OH, superoxide radical ($O2^{\cdot -}$), singlet oxygen (1O2), and oxygen vacancies, respectively. A mixture of 0.5 mL Cu-N/C aqueous solution (0.5 mg/mL), 1 mL 4-AP (1 mM), and 1 mL 2,4-DP (1 mM) was added to 0.5 mL MES buffer (60 mM)

containing different scavengers. The reaction was conducted at 25 °C for 40 min. Afterward, the suspension was collected and analyzed by UV–Vis spectrophotometry at 510 nm.

1.5 Detection of phenols and amines

Phenol solutions at concentrations of 20, 50, 100, 200, 300, 400, and 500 μM were mixed with 0.5 mL of Cu-N/C in water (0.5 mg·mL-1) and 1 mL of 4-AP (1 mM) in 0.5 mL of MES buffer (60 mM, pH = 7.0) for 40 minutes at 25 °C. The progress of the reaction was monitored by measuring the absorbance of the supernatant at 510 nm. The limit of detection is calculated by 3σ/b, where σ represents the standard deviation of the blank sample and b represents the slope of the standard curve. The detection process for p-chlorophenol is similar to the above.

To evaluate the catalytic performance of Cu-N/C against amine compounds, 0.5 mL of Cu-N/C aqueous dispersion (0.5 mg·mL-1) was mixed with 1 mL of aqueous o-phenylenediamine and 1.5 mL of MES buffer (60 mM, pH = 7.0) for 40 minutes at 25 °C. The concentrations of o-phenylenediamine were 100, 300, 500, 700, 800, 900, and 1000 μM, respectively. A standard curve was established by the concentration of o-phenylenediamine and its absorbance at 418 nm.

2. Supplementary Figure S1-S9 and Table S1-S2

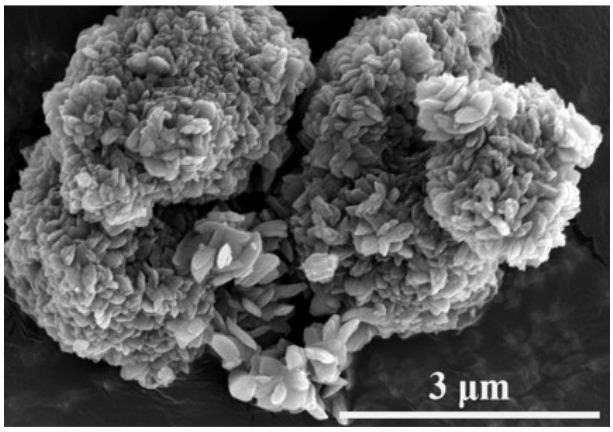

Figure S1. (a) SEM images of Cu-phen.

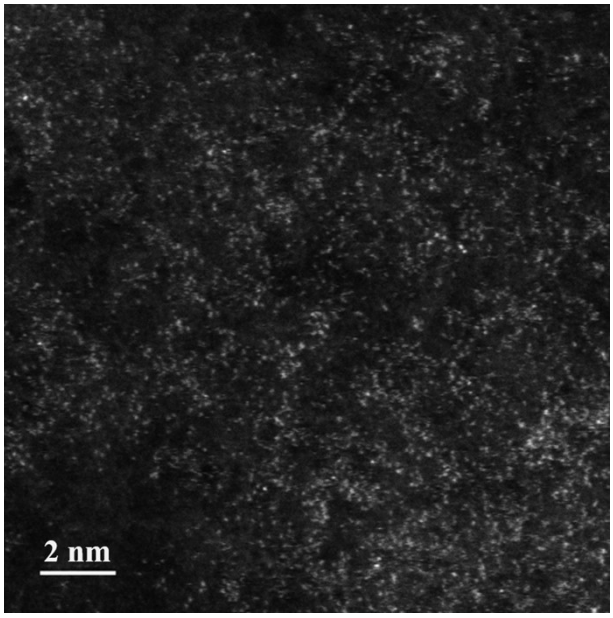

Figure S2.AC-HAADF-STEM images of Cu-N/C.

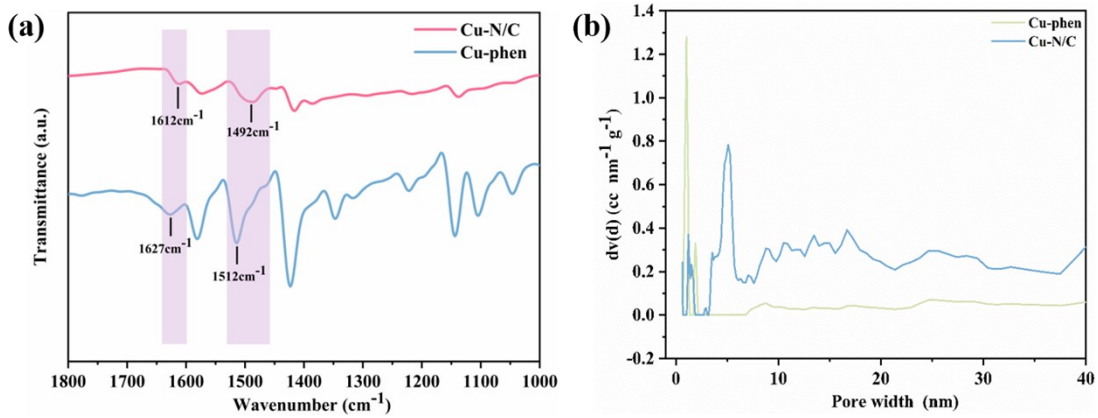

Figure S3. (a) FT-IR spectra of Cu-phen and Cu-N/C. (b) Pore size distributions of Cu-phen and Cu-N/C.

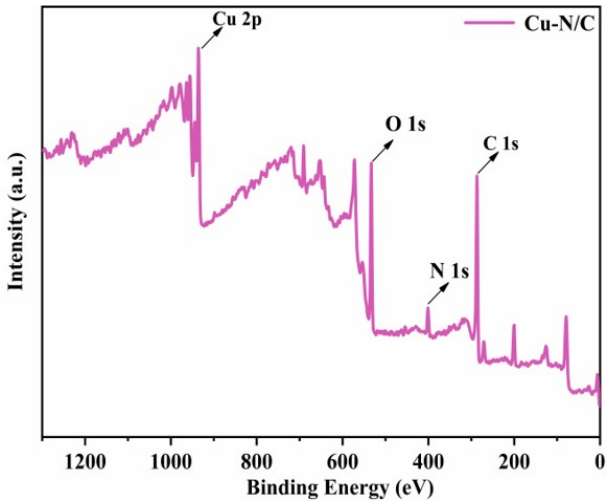

Figure S4. The full XPS spectra of Cu-N/C.

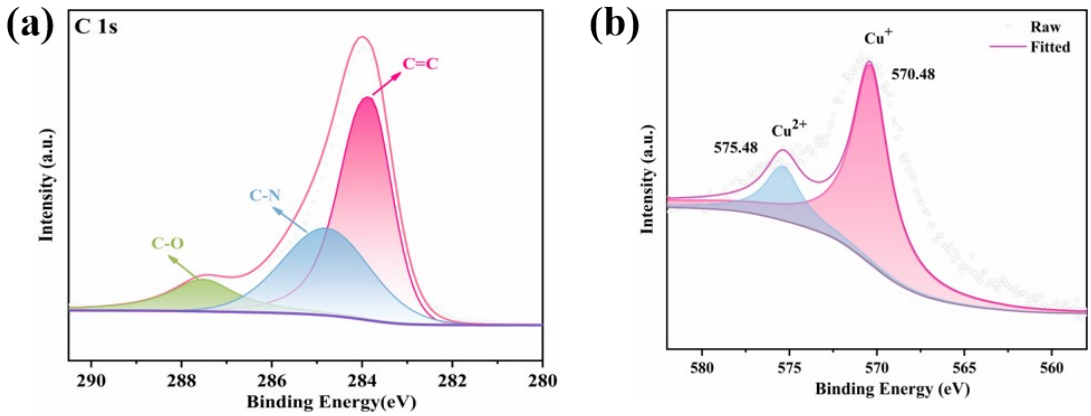

Figure S5. (a) High-resolution C 1s XPS spectra of Cu-N/C.
(b) Cu LMM Auger spectrum.

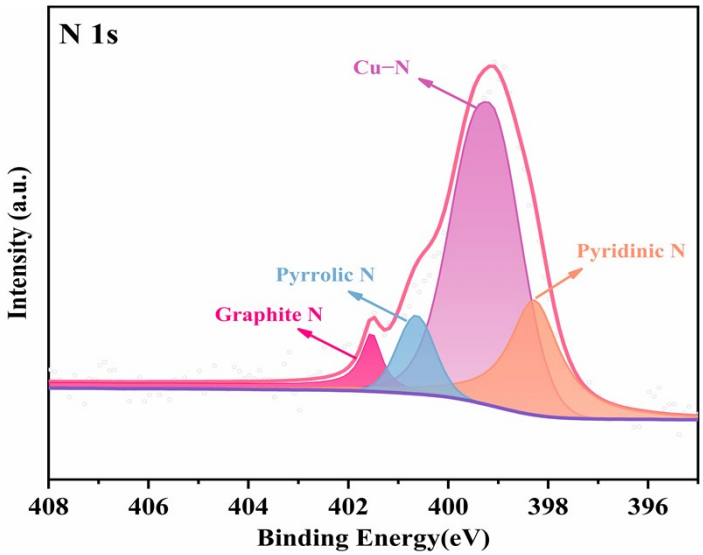

Figure S6. N 1s XPS spectra of Cu-N/C.

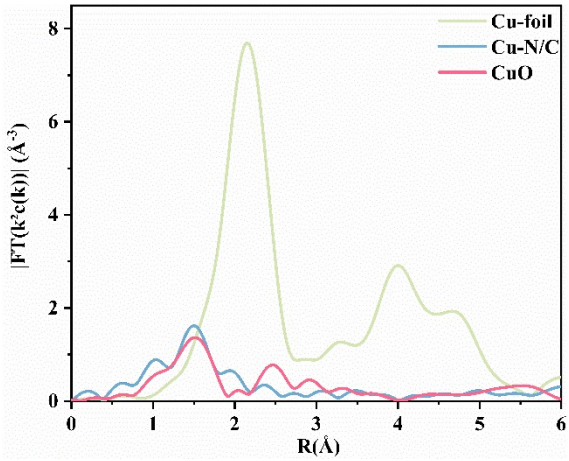

Figure S7. K-edge EXAFS of different samples with Cu.

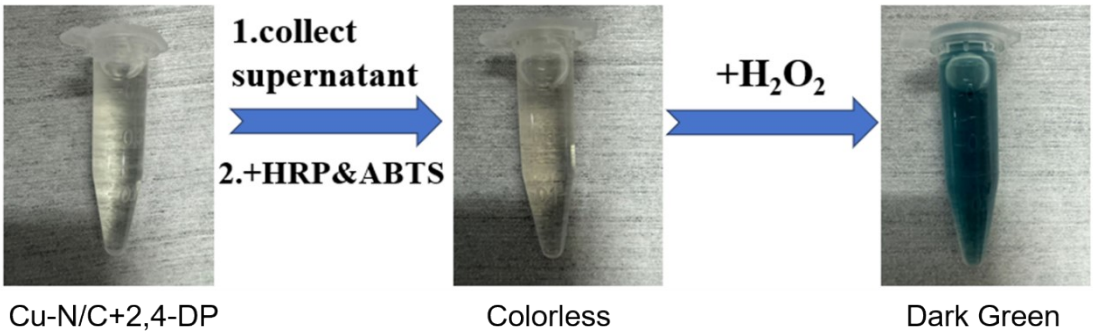

Figure S8. Photos of the hydrogen peroxide test results.

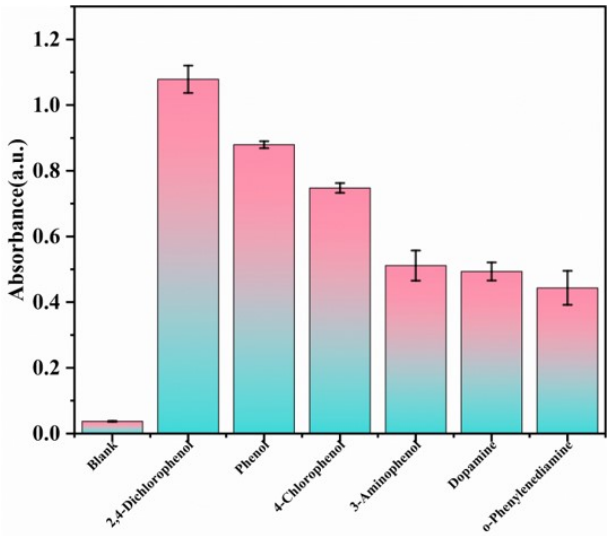

Figure S9. The catalytic selectivity of Cu-N/C for different substrates.

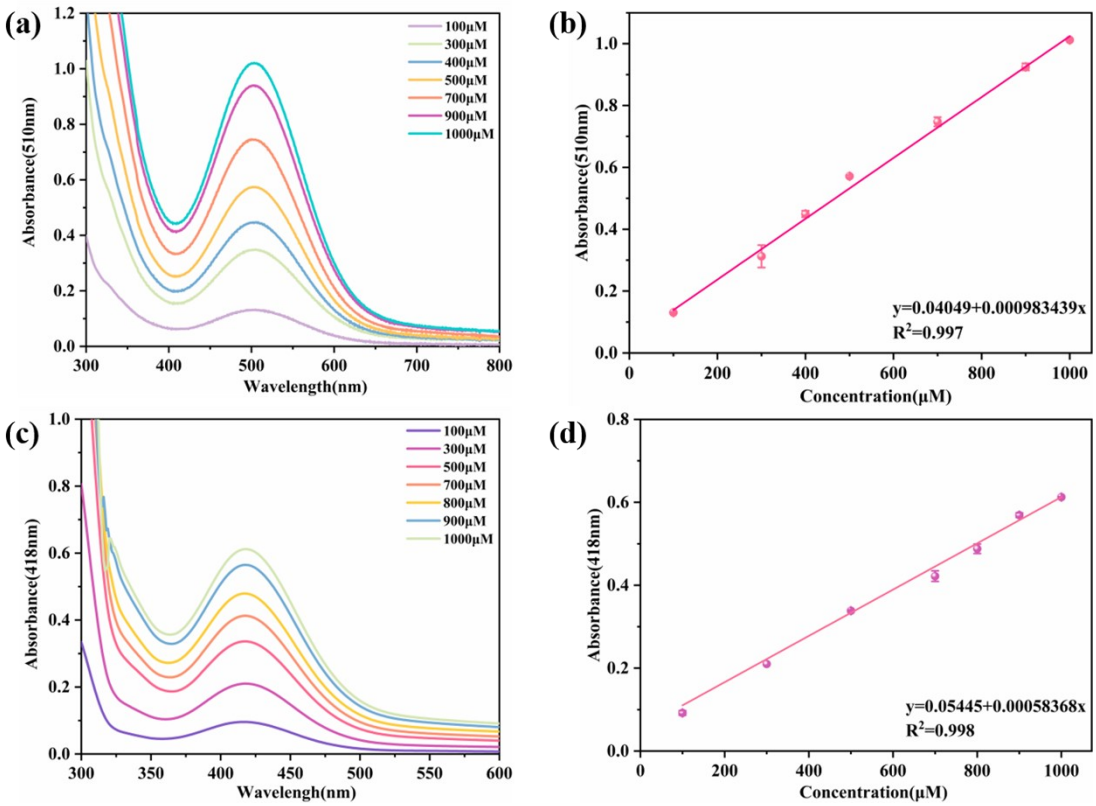

Figure S10. (a) UV-vis spectra of the Cu-N/C catalytic system using 4-chlorophenol as substrate at pH 7.0; (b) Linear relationship between 4-chlorophenol concentration and absorbance; (c) UV-vis spectra of o-phenylenediamine oxidation products in MES buffer (60 mM, pH 7.0); (d) Linear relationship between o-phenylenediamine concentration and absorbance.

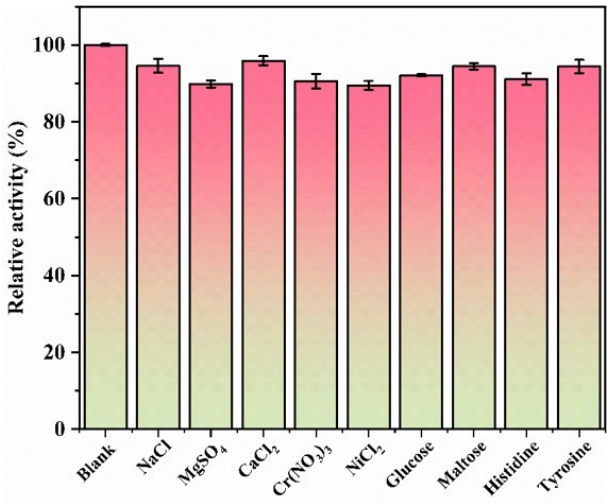

Figure S11. Interference resistance of Cu-N/C nanozyme to potential interfering substances.

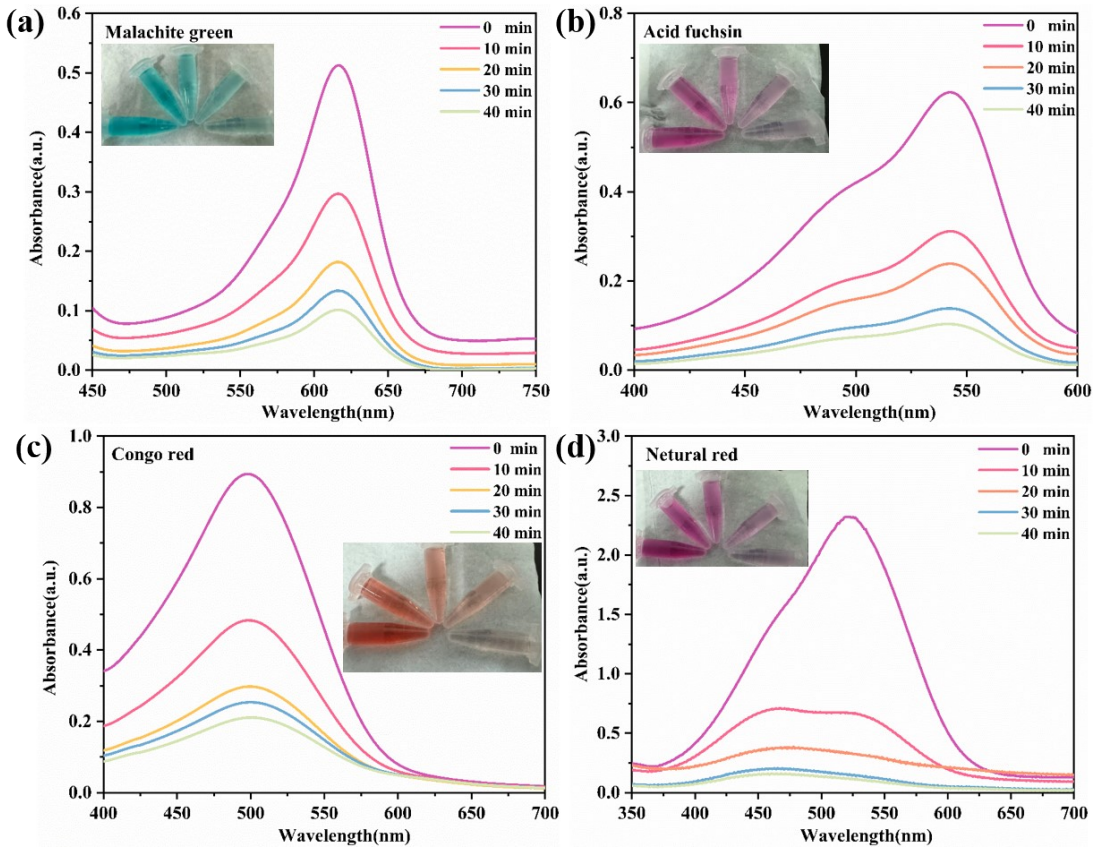

Figure S12. UV-Vis absorption spectra of four dyes, including (a) malachite green, (b) acidic fuchsin, (c) congo red, (d) neutral red, in the presence of Cu-N/C, for 40 minutes.

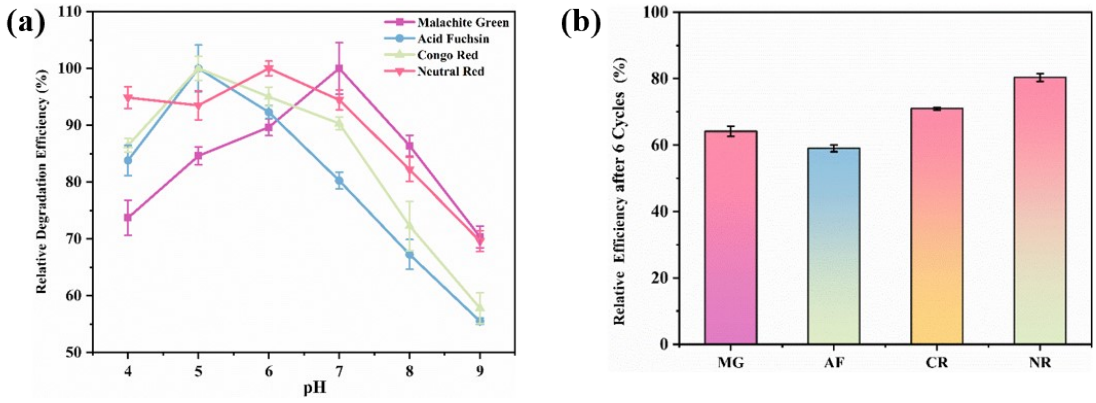

Figure S13. (a) The effect of pH on dye degradation. (b) Comparison of relative efficiency after cycling.

Table S1 Elemental percentage content

Elements	Atomic percentage (%)
C	60.58
Cu	21.76
O	10.85
N	6.81

Table S2. Porosity parameters

Sample	Surface Area(m^2 /g)	Pore Volume(cm^3 /g)	Pore Width (Mode, nm)
Cu-phen	405.994	0.229	1.022
Cu-N/C	609.680	0.467	5.102

Table S3. Comparison of laccase - like catalytic kinetic parameters of Cu – N/C, free laccase and other reported laccase mimics

Catalyst	K_m (mM)	V_{max} (mM min^{-1})	Ref.
Cu-NH_2-BDC-Mel	0.19	1.79×10^{-3}	1
Tris-Cu	0.18	15.62×10^{-3}	2
CH-Cu	0.42	7.32×10^{-3}	3
BpA-Cu	0.070	1.56×10^{-3}	4
Cu/GMP	0.59	0.83×10^{-3}	5
I-Cu	0.17	0.41×10^{-3}	6
His-Cys-Cu	1.53	2.85×10^{-3}	7
CA-Cu	0.23	0.0030×10^{-3}	8
Laccase	0.52	5.12×10^{-4}	This work
Cu-N/C	0.096	1.30×10^{-3}	This work

Table S4. Comparison of various testing approaches for phenol

Materials	Linear range	Detection limit	Detection method	Reference
SPE/E-rGO	1–40 μM	0.20 μM	Electrochemical	9
CeO_2 microstructures	1.1-527.6 μM	0.38 μM	Electrochemical	10
Supramolecular solvent	0.11-1.59 μM	0.021 μM	HPLC	11
Fe_1@CN-20	160-532 μM	2.60 μM	Colorimetric	12
Fe_3O_4/CNC@MOF	2-200 μM	0.32 μM	Colorimetric	13
AMP-Cu	0.1–100 μM	0.033 μM	Colorimetric	14
Cu-N/C	50-500 μM	0.060 μM	Colorimetric	This work

Table S5. Analysis of added phenol in actual water samples

Sample	Added (μM)	Found (μM)	Recovery (%)	RSD (%, n = 3)
Drinking water	50	50.81±1.67	101.62	3.28
	200	201.87 ± 4.33	100.94	2.15
	500	499.61 ± 2.80	99.92	0.56
Tap water	50	49.47±0.80	98.94	1.62
	200	200.94 ± 2.44	100.47	1.21
	500	501.74 ± 4.40	100.35	0.88
Xianlin lake	50	50.27±0.80	100.54	1.59
	200	199.16 ± 8.12	99.58	4.08
	500	503.87 ± 4.80	100.77	0.95

Table S6. Comparison of Cu-N/C with other reported catalysts

Catalyst	Concentration Catalyst (mg/mL)	Dye	Degradation efficiency (%)	Time (min)	Reference
3DOM Fe-N-C	0.018	RhB	92	240	15
Mn-SAzyme	0.025	MB	90.1%	300	16
CeO_2@ZIF-8	5.0	Five dyes	Above 80	360	17
Cu–TiO_2 NT	——	MO	80	300	18
Mn-GMPNS	0.5	Six dyes	Above 70	30	19
MnO_2/Cu-BDC-His	0.2	Four dyes	Above 80	20	20
Cu-N/C	3.0	Four dyes	Above 75	40	This work

Supporting References

1. H. Qiao, H. Yang, Y. Han, Y. Liu, Y. Zhang and X. Zhang, Excellent laccase-like activity of melamine modified Cu-NH_2-BDC and selective sensing analyses toward phenols and amines, *Nano Research*, 2024, **17**, 9887-9897.
2. T. Q. Chai, J. L. Wang, G. Y. Chen, L. X. Chen and F. Q. Yang, Tris-Copper Nanozyme as a Novel Laccase Mimic for the Detection and Degradation of Phenolic Compounds.*Journal*, 2023, **23**.
3. J. Wang, R. Huang, W. Qi, R. Su, B. P. Binks and Z. He, Construction of a bioinspired laccase-mimicking nanozyme for the degradation and detection of phenolic pollutants, *Applied Catalysis B: Environmental*, 2019, **254**, 452-462.
4. Y. Liu, L. Liu, Z. Qu, L. Yu and Y. Sun, Supramolecular assembly of benzophenone alanine and copper presents high laccase-like activity for the degradation of phenolic pollutants, *Journal of Hazardous Materials*, 2023, **443**, 130198.
5. A. H. Memon, R. Ding, Q. Yuan, H. Liang and Y. Wei, Coordination of GMP ligand with Cu to enhance the multiple enzymes stability and substrate specificity by co-immobilization process, *Biochemical Engineering Journal*, 2018, **136**, 102-108.
6. J. Wang, R. Huang, W. Qi, R. Su and Z. He, Construction of biomimetic nanozyme with high laccase- and catecholase-like activity for oxidation and detection of phenolic compounds, *Journal of Hazardous Materials*, 2022, **429**, 128404.
7. X. Yan, H. Li, T. Wang, A. Li, C. Zhu and G. Lu, Engineering of coordination environment in bioinspired laccase-mimicking catalysts for monitoring of pesticide poisoning, *Chemical Engineering Journal*, 2022, **446**, 136930.
8. J. Wang, R. Huang, W. Qi, R. Su and Z. He, Preparation of amorphous MOF based biomimetic nanozyme with high laccase- and catecholase-like activity for the degradation and detection of phenolic compounds, *Chemical Engineering Journal*, 2022, **434**, 134677.
9. S. Singh, N. Kumar, V. K. Meena, C. Kranz and S. Mishra, Impedometric phenol sensing using graphenated electrochip, *Sensors and Actuators B: Chemical*, 2016, **237**, 318-328.
10. X. Xiao, W. YiHui, Z. DongEn, G. JunYan, M. JuanJuan, Y. Tao and Z. and Tong, Synthesis of pumpkin-like CeO_2 microstructures and electrochemical detection for phenol, *Inorganic and Nano-Metal Chemistry*, 2019, **49**, 349-353.
11. Y. Lu, L. Yan, Y. Wang, S. Zhou, J. Fu and J. Zhang, Biodegradation of phenolic compounds from coking wastewater by immobilized white rot fungus Phanerochaete chrysosporium, *Journal of Hazardous Materials*, 2009, **165**, 1091-1097.
12. Y. Lin, F. Wang, J. Yu, X. Zhang and G.-P. Lu, Iron single-atom anchored N-doped carbon as a 'laccase-like'

nanozyme for the degradation and detection of phenolic pollutants and adrenaline, *Journal of Hazardous Materials*, 2022, **425**, 127763.
13. C. Hou, L. Fu, Y. Wang, W. Chen, F. Chen, S. Zhang and J. Wang, Core–shell magnetic Fe_3O_4/CNC@MOF composites with peroxidase-like activity for colorimetric detection of phenol, *Cellulose*, 2021, **28**, 9253-9268.
14. H. Huang, L. Lei, J. Bai, L. Zhang, D. Song, J. Zhao, J. Li and Y. Li, Efficient elimination and detection of phenolic compounds in juice using laccase mimicking nanozymes, *Chinese Journal of Chemical Engineering*, 2021, **29**, 167-175.
15. S. Wu, W. Wu, X. Zhu, M. Li, J. Zhao and S. Dong, Atomically dispersed hierarchically ordered porous Fe-N-C single-atom nanozymes for dyes degradation, *Nano Research*, 2023, **16**, 10840-10847.
16. Q. Feng, G. Wang, L. Xue, Y. Wang, M. Liu, J. Liu, S. Zhang and W. Hu, Single-Atom Nanozyme Based on Mn-Center with Enhanced Peroxidase-like Activity for Organic Dye Degradation, *ACS Applied Nano Materials*, 2023, **6**, 4844-4853.
17. T. H. Yang, X. F. Liu, Z. H. Zeng, X. J. Wang, P. Zhang, B. Feng, K. Tian and T. P. Qing, Efficient and recyclable degradation of organic dye pollutants by CeO_2@ZIF-8 nanozyme-based non-photocatalytic system, *ENVIRONMENTAL POLLUTION*, 2023, **316**.
18. S. Sreekantan, S. M. Zaki, C. W. Lai and T. W. Tzu, Post-annealing treatment for Cu-TiO_2 nanotubes and their use in photocatalytic methyl orange degradation and Pb(II) heavy metal ions removal, *EUROPEAN PHYSICAL JOURNAL-APPLIED PHYSICS*, 2014, **67**.
19. Q. Tang, C. Zhou, L. Shi, X. Zhu, W. Liu, B. Li and Y. Jin, Multifunctional Manganese–Nucleotide Laccase-Mimicking Nanozyme for Degradation of Organic Pollutants and Visual Assay of Epinephrine via Smartphone, *Analytical chemistry*, 2024, **96**, 4736-4744.
20. M. Li, Y. Xie and X. Su, Versatile laccase-mimicking enzyme for dye decolorization and tetracyclines identification upon a colorimetric array sensor, *Journal of Hazardous Materials*, 2025, **483**, 136683.